Journal of Alloys and Compounds 509 (2011) 2540–2543

Contents lists available at ScienceDirect

Journal of Alloys and Compounds

journal homepage: www.elsevier.com/locate/jallcom

Intense blue photoluminescence of the Tm^{3+}/Yb^{3+} co-doped single-crystalline hexagonal phase $NaYF_4$ nanorods

Songjun Zeng*, Guozhong Ren, Changfu Xu

Institute of Modern Physics, Xiangtan University, Xiangtan 411105, China

ARTICLE INFO

Article history:
Received 31 August 2010
Received in revised form
11 November 2010
Accepted 11 November 2010
Available online 21 November 2010

Keywords:
Nanorods
Hydrothermal method
Hexagonal phase
Upconversion

ABSTRACT

In this paper, Tm^{3+}/Yb^{3+} co-doped $NaYF_4$ single-crystalline nanorods were prepared via a rational hydrothermal method using oleic acid as a stabilizing agent. The microstructure analysis revealed that the as-prepared samples presented a pure hexagonal phase $NaYF_4$ structure with high quality rod-like morphology by means of X-ray diffraction (XRD) and transmission electron microscopy (TEM). Under 980 nm excitation, the intense blue and weaker red upconversion emissions of the $NaYF_4$: 1%Tm^{3+}/x%Yb^{3+} (x = 2, 5, 10 and 15) samples centered at 450, 477, 649 and 690 nm were observed, which were attributed to the $^1D_2 \rightarrow {}^3F_4$, $^1G_4 \rightarrow {}^3H_6$, $^1G_4 \rightarrow {}^3F_4$ and $^3F_3 \rightarrow {}^3H_6$ transitions of Tm^{3+}, respectively. Moreover, the photograph of the 1%Tm^{3+}/10%Yb^{3+} co-doped $NaYF_4$ nanorods exhibited a strong eye-visible blue emission. The upconversion luminescence mechanisms for the Tm^{3+}/Yb^{3+} co-doped hexagonal phase $NaYF_4$ nanorods were analyzed. In addition, the effect of Yb^{3+} ions concentrations on the photoluminescence properties of the Tm^{3+}/Yb^{3+} co-doped hexagonal phase $NaYF_4$ nano-rods were investigated in detail.

1. Introduction

In recent years, the rare earth (RE) doped optical materials have been extensively investigated due to their potential applications in many fields, such as color display, optical data storage, sensor, laser and optical amplifier for communication [1–5]. Upconversion is the generation of higher energy light such as ultraviolet or visible light from lower energy radiation, usually near-infrared or infrared via two photon or multi-photon mechanism [6]. It is well known that, as the host for the luminescent RE, fluoride is preferable over oxide mainly for the lower phonon energy to avoid non-radiative transition of RE ions [7]. To the best of our knowledge, among the reported fluoride upconversion materials, hexagonal phase $NaYF_4$ is one of the most efficient upconversion host material for visible upconversion luminescence [8]. In recent years, one dimensional nanoscale materials, such as nanowires, nanotubes, nanobelts and nanorods, have attracted much interest due to their potential applications in fabricating nanoscale optoelectronics [9,10], electronics [11,12], lasers [9,13] and biological labels [14], etc. Many unique and fascinating properties have already been demonstrated for this kind of materials, such as high luminescence efficiency, enhancement of thermoelectric figure of merit and a lowered lasing threshold [15,16]. Hence, it is important to synthesize highly uniform and monodispersed hexagonal phase $NaYF_4$ nanocrystals with one dimensional rod-shaped structure, as mentioned above. However, most of the previous reports were mainly focused on the preparation of $NaYF_4$ nano- and micro-crystals morphologies [17–22]. Only limited reports were devoted to synthesizing hexagonal phase $NaYF_4$ nanocrystals with rod-like shape. In this paper, Tm^{3+}/Yb^{3+} co-doped hexagonal phase $NaYF_4$ single-crystalline nanorods with high quality were prepared via a rational hydrothermal method using oleic acid as a stabilizing agent. Intense blue emission can be achieved from this Tm^{3+}/Yb^{3+} co-doped hexagonal phase $NaYF_4$ nanorods. And the effect of Yb^{3+} concentrations on upconversion property of the 1%Tm^{3+}/x%Yb^{3+} (x = 2, 5, 10 and 15) co-doped hexagonal phase $NaYF_4$ single-crystalline nanorods was studied in detail.

2. Experimental

The Tm^{3+}/Yb^{3+} co-doped $NaYF_4$ nanorods were prepared with the following compositions (in mol %): $NaYF_4$: 1%Tm^{3+}/x%Yb^{3+} (x = 2, 5, 10 and 15). All the rare-earth oxides were 99.99% purity and other raw materials are of analytical reagent grade. Rare earth nitrate $RE(NO_3)_3$ (RE = Y, Yb and Tm) solutions with 0.5 mol L^{-1}, 0.5 mol L^{-1} and 0.1 mol L^{-1} were prepared by dissolving the corresponding rare earth oxide (99.99%) in nitric acid at elevated temperature respectively and excess nitric acid was removed by evaporation. A typical synthesis of Tm^{3+}/Yb^{3+} co-doped $NaYF_4$ nanorods were performed by a rational hydrothermal method using oleic acid as a stabilizing agent [23,24–26]. For a typical synthesis, 1.2 g NaOH, 2 mL distilled water, 9 mL ethanol, and 20 mL oleic acid were mixed together under vigorously stirring to form a homogeneous solution. Next, 1 mmol (total amounts) of $RE(NO_3)_3$ (RE = Y, Yb and Tm) and 8 mL NaF (1.0 M) aqueous solution were added to the solution under vigorously stirring. The resulting mixture was stirred for another 30 min. The resulting solution was then transferred into a 50 mL stainless Teflon-lined autoclave, sealed, and heated at 190 °C for 24 h. The system was then allowed to cool down to room temperature naturally and the products were deposited at the bottom of the vessel. The final products can be well-dispersed

* Corresponding author. Tel.: +86 0732 8292113.
E-mail address: songjunz@xtu.edu.cn (S. Zeng).

0925-8388/$ – see front matter © 2010 Elsevier B.V. All rights reserved.
doi:10.1016/j.jallcom.2010.11.084

in a nonpolar solvent such as cyclohexane and aggregated by adding polar solvent such as ethanol. The obtained nanorods were washed with ethanol and water to remove oleic acid and other remnants, and then dried in air at 60 °C for 6 h.

The crystal phase of the as-obtained samples was recorded by a D/max-γA System X-ray diffractometer at 40 kV and 40 mA with Cu-Kα radiation (λ = 0.15418 nm). The scan was performed in the 2θ range from 5°–80° with a scanning rate of 0.04°/s and step size of 0.04°. The morphology and microstructure of the as-prepared samples were further characterized by TEM and the high resolution transmission electron microscopy (HRTEM) assays using a JEM-2100 microscope operated at 200 kV. The upconversion emission spectra at room temperature were recorded by a spectrophotometer (R500) under the excitation of 980 nm laser diode (LD). All the above measurements were carried out at room temperature.

3. Results and discussion

$NaYF_4$ exists in two polymorphs at ambient pressure: cubic phase and hexagonal phase. The phase compositions of the as-prepared products were detected by the powder XRD pattern. The XRD pattern of $NaYF_4$: 1% Tm^{3+}, 10% Yb^{3+} samples obtained from the hydrothermal condition at 190 °C for 24 h is shown in Fig. 1. The peak positions and intensities of the XRD pattern matched well with the reference hexagonal phase $NaYF_4$ (JCPDS 16-0334). No other impurity peaks were detected. In addition, the well-defined diffraction peaks demonstrated that the as-prepared samples had high crystalline nature. Similar results were observed for the 1% Tm^{3+}/x%Yb^{3+} (x = 2, 5 and 15) doped samples. However, the preferred growth direction of the nanorods is not directly reflected in the XRD patterns, which may be related to the relative small aspect ratio of the nanorods.

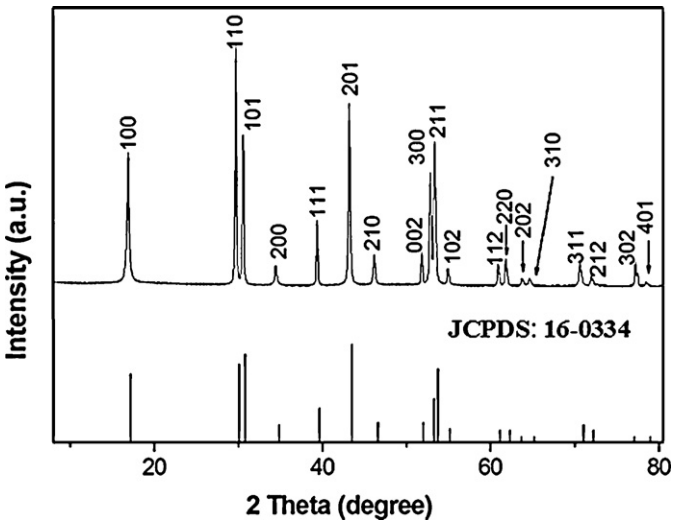

Fig. 1. Typical XRD pattern of the as-synthesized $NaYF_4$: 1%Tm^{3+}/10%Yb^{3+} nanorods.

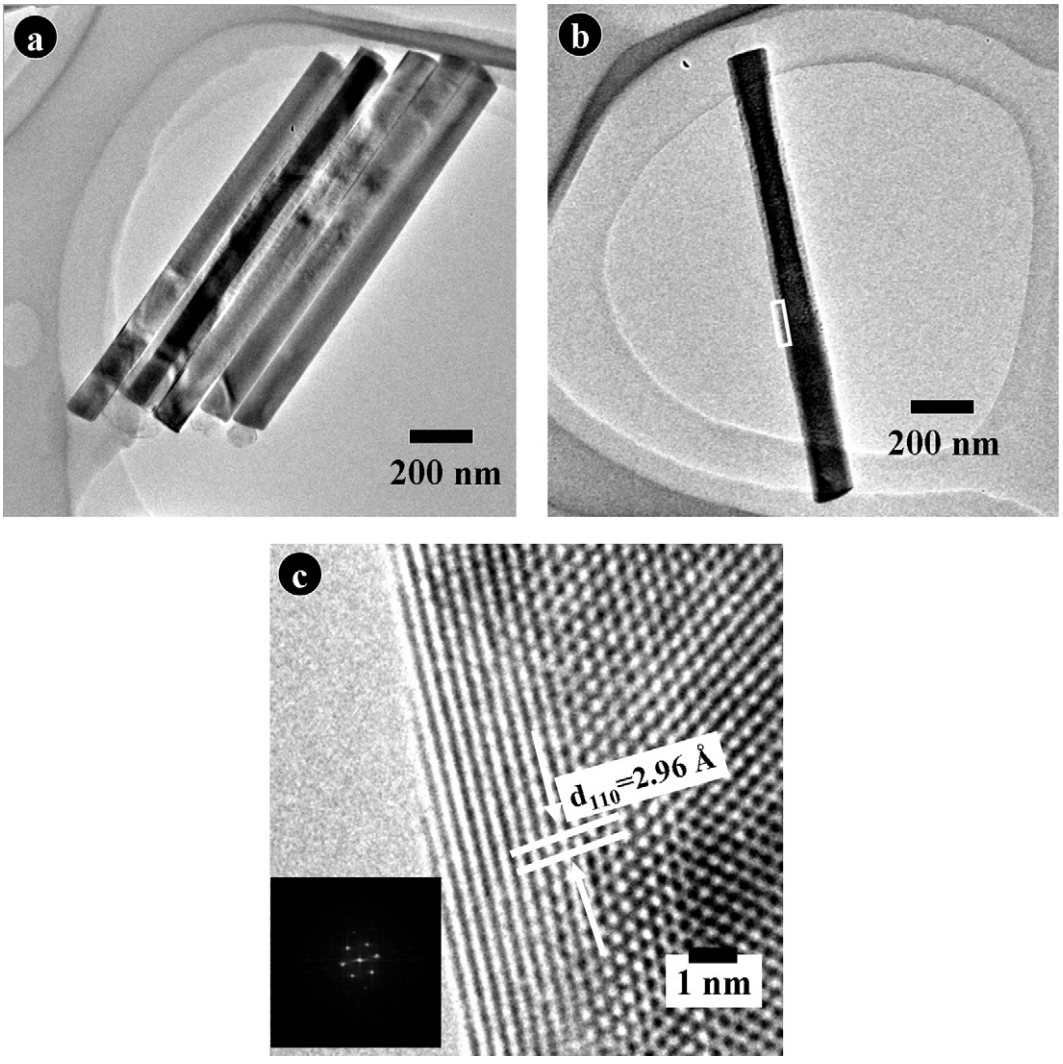

Fig. 2. The typical TEM and HRTEM images of the $NaYF_4$: 1%Tm^{3+}/10%Yb^{3+} nanorods: (a) low magnification image, (b) the individual nanorod, (c) the corresponding HRTEM image taken from the area marked by a white rectangle. The inset of (c) is the corresponding FFT image.

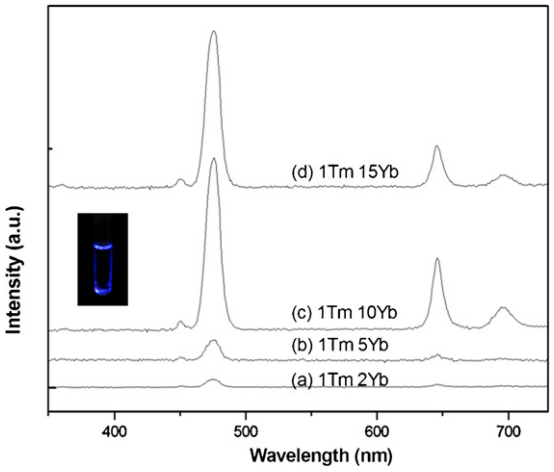

Fig. 3. Dependence of upconversion emission spectra on Yb^{3+} concentration of $NaYF_4$: 1%Tm^{3+}/x%Yb^{3+} samples: (a) 1 mol%Tm^{3+}, 2 mol%Yb^{3+} ions; (b) 1 mol%Tm^{3+}, 5 mol%Yb^{3+}; (c) 1 mol%Tm^{3+}, 10 mol%Yb^{3+}; (d) 1 mol%Tm^{3+}, 15 mol%Yb^{3+}. The inset shows the photograph of 1 wt% colloidal solution of as-prepared $NaYF_4$: 1%Tm^{3+}/10%Yb^{3+} samples dispersed in cyclohexane under the excitation of 980 nm excitation laser diode with power density of 3 W/cm^2.

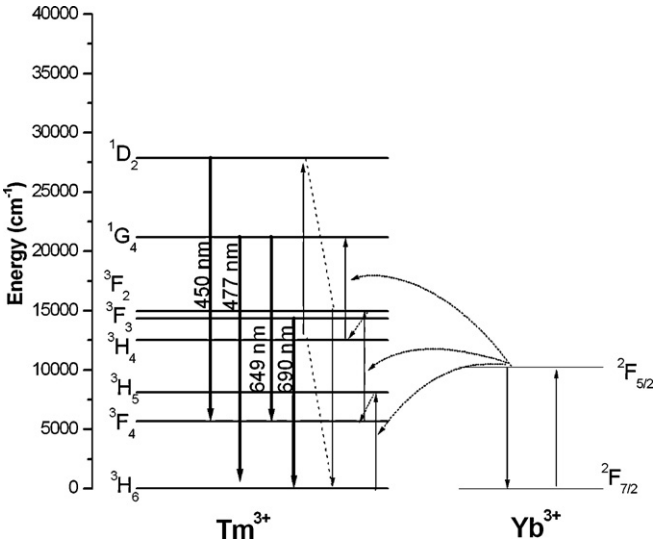

Fig. 4. Simplified energy-level diagram of Tm^{3+} and Yb^{3+}.

The morphology and microstructure of the samples were characterized by TEM and HRTEM. Fig. 2a showed the typical TEM image of the as-prepared $NaYF_4$: 1% Tm^{3+}/10%Yb^{3+} samples and Fig. 2b is the typical TEM image of an individual $NaYF_4$ nanorod. From these TEM observations, it can be seen that the sample exhibits rod-like morphology with smooth wall. Furthermore, these nanorods display uniform morphology and high quality. The length of the as-prepared nanorods is about 1500 nm and the diameter is about 90 nm, as estimated from the TEM images, and the aspect ratio is about 16. Fig. 2c shows the typical HRTEM image taken from the white rectangle area of the individual nanorod. As demonstrated in Fig. 2c, the as-prepared $NaYF_4$ nanorods exhibited highly crystalline nature, which is structural uniformity and free of the defects. The measured interplanar distance is about 2.96 Å, corresponding to the (1 1 0) lattice plane of the hexagonal phase $NaYF_4$, which is consistent with the XRD result. The inset of Fig. 2c is the corresponding fast fourier transform (FFT) image. The regular diffraction spots of FFT image recorded along the [0 0 1] zone axis unambiguously demonstrate the single nanorod has single-crystalline nature. The diffraction pattern can be readily indexed as the hexagonal phase $NaYF_4$, which is also well consistent with the XRD analysis. Based on the HRTEM analysis, the preferred growth direction of the as-prepared nanorods is along the [1 1 0] direction.

The upconversion photoluminescence of different compositions of Tm^{3+}/Yb^{3+} co-doped hexagonal phase $NaYF_4$ nanorods are shown in Fig. 3. Under the excitation of a 980 nm LD, the blue and red emissions centered at 450, 477, 649 and 690 nm were observed, which were attributed to the $^1D_2 \rightarrow {}^3F_4$, $^1G_4 \rightarrow {}^3H_6$, $^1G_4 \rightarrow {}^3F_4$ and $^3F_3 \rightarrow {}^3H_6$ transitions of Tm^{3+}, respectively. The inset of Fig. 3c shows the photograph of 1 wt% colloidal solution of as-prepared $NaYF_4$: 1%Tm^{3+}/10%Yb^{3+} nanorods dispersed in cyclohexane under the excitation of 980 nm LD with power density of 3 W/cm^2. As demonstrated in the photography image, the bright blue upconversion luminescence can be observed by naked eyes. It is also noted that the intensities of these bands increase with increasing the concentration of Yb^{3+} and further decrease when the concentration of Yb^{3+} ions reaches at 15 mol%, which may be attributed to the concentration quenching [27]. According to the simplified energy level diagram shown in Fig. 4, the possible upconversion mechanisms have been discussed in detail. Excitation photons (λ = 980 nm) are strongly absorbed by isolated Yb^{3+} ions because Yb^{3+} ions have larger absorption cross section and Tm^{3+} ions have no corresponding energy level. These ions act as sensitizers and this absorption process is strongly dependent on the distance between neighboring ions. After absorption of photons by Yb^{3+}, energy transfer (ET) takes place between Yb^{3+} and Tm^{3+}. Under 980 nm excitation, the Yb^{3+} ions are excited from the $^2F_{7/2}$ level to the $^2F_{5/2}$ level, then transfer their energies to the nearby Tm^{3+} ions, then three successive ET from Yb^{3+} to Tm^{3+} populate the $^3H_5$, $^3F_2$, and $^1G_4$ levels of Tm^{3+} [28]. Consequently, the blue emission centered at 477 nm is generated by the $^1G_4 \rightarrow {}^3H_6$ transition of Tm^{3+} ions. While, the red emissions at 649 and 690 nm are due to the $^1G_4 \rightarrow {}^3F_4$ and $^3F_3 \rightarrow {}^3H_6$ transitions of Tm^{3+} ions, respectively. Due to the large energy mismatch between $^1G_4$ and $^1D_2$ levels of Tm^{3+} (about 3500 cm^{-1}), the $^1G_4 \rightarrow {}^1D_2$ transition of Tm^{3+} cannot be directly achieved by the absorption of the fourth photon from Yb^{3+} via ET process. Therefore, the cross relaxation (CR) process of $^3F_2$+$^3H_4 \rightarrow {}^3H_6$+$^1D_2$ between Tm^{3+} ions may alternatively play an important role in populating $^1D_2$ level [29,30], which subsequently resulting in the blue emission band centered at 450 nm. However, compared with the blue emission band centered at 477 nm, the intense of the blue emission centered at 450 nm is much weaker, which is ascribed to the poor CR process of Tm^{3+} ions.

4. Conclusions

A series of 1%Tm^{3+}/x%Yb^{3+} (x = 2, 5, 10, 15) co-doped hexagonal phase $NaYF_4$ single-crystal nanorods with high quality were fabricated by a facile hydrothermal method. The intense blue emission centered at 477 nm of Tm^{3+}/Yb^{3+} co-doped hexagonal phase $NaYF_4$ nanorods were observed under the excitation of a 980 nm laser diode. The influence of Yb^{3+} concentration on all the emissions is obvious, which indicates the Yb^{3+} ion plays an important role in the energy transfer process. With increasing the Yb^{3+} contents, the upconversion emission intensity gradually increased. However, it decreased when the doping of Yb^{3+} reached to 15 mol%, owing to the effect of concentration quenching. More importantly, the intense eye-visible blue luminescence can be observed from the 1%Tm^{3+}/10%Yb^{3+} co-doped $NaYF_4$ nanorods under the excitation of a 980 nm laser diode with power density of 3 W/cm^2. It is therefore expected that these single-crystal and high quality one-dimensional nanorods with intense eye-visible blue upconversion luminescence may have potential applications in visible solid-state lasers and biolabels.

Acknowledgments

This work is supported by the National Natural Scientific Foundation of China (No. 10874144) and the Scientific Foundation of Education Department of Hunan Province (No. 08C885)

References

[1] J.S. Wang, E.M. Vogel, E. Snitzer, Opt. Mater. 3 (1994) 187.
[2] D. Chen, Y.S. Wang, F. Bao, Y. Yu, J. Appl. Phys. 101 (2007) 113511.
[3] Y. Kishi, S. Tanabe1, S. Tochino, G. Pezzotti, J. Am. Ceram. Soc. 88 (2005) 3423.
[4] S. Tanabe, H. Hayashi, T. Hanada, N. Onodera, Opt. Mater. 19 (2002) 343.
[5] Y.H. Liu, Y.J. Chen, Y.F. Lin, Q.G. Tan, Z.D. Luo, Y.D. Huang, J. Opt. Soc. Am. B: Opt. Phys. 24 (2007) 1046.
[6] F. Auzel, Chem. Rev. 104 (2004) 139.
[7] M. Abril, J. Méndez-Ramos, I. Martín, U. Rodríguez-Mendoza, V. Lavín, A. Delgado-Torres, V.D. Rodríguez, J. Appl. Phys. 95 (2004) 5271.
[8] K.W. Kramer, D. Biner, G. Frei, H.U. Gudel, M.P. Hehlen, S.R. Luthi, Chem. Mater. 16 (2004) 1244.
[9] X.F. Duan, Y. Huang, R. Agarwal, C.M. Lieber, Nature 421 (2003) 241.
[10] X.D. Wang, C.J. Summers, Z.L. Wang, Nano lett. 4 (2004) 423.
[11] J. Cao, Q. Wang, H. Dai, Nat. Mater. 4 (2005) 745.
[12] A. Javey, H. Kim, M. Brink, Q. Wang, A. Ural, J. Guo, P. Melntyre, P. Mceuen, M. Lundstrom, H. Day, Nat. Mater. 1 (2002) 241.
[13] J.C. Johnson, H.J. Choi, K.P. Knutsen, R.D. Schaller, P.D. Yang, R.J. Saykally, Nat. Mater. 1 (2002) 106.
[14] J.H. Zeng, J. Sun, Z.H. Li, R.X. Yan, Y.D. Li, Adv. Mater. 17 (2005) 2119.
[15] M.H. Huang, S. Mao, H. Feick, H.Q. Yan, Y.Y. Wu, H. Kind, E. Weber, R. Russo, P.D. Yang, Science 292 (2001) 1897.
[16] L.D. Hicks, M.S. Dresselhaus, Phys. Rev. B 47 (1995) 16631.
[17] M. Wang, C.C. Mi, J.L. Liu, X.L. Wu, Y.X. Zhang, W. Hou, F. Li, S.K. Xu, J. Alloys Compd. 485 (2009) L24.
[18] G.F. Wang, W.P. Qin, J.S. Zhang, L.L. Wang, G.D. Wei, P.F. Zhu, R.J. Kim, J. Alloys Compd. 475 (2009) 452.
[19] S.Y. Tan, P.P. Yang, N. Niu, S.L. Gai, J. Wang, X.Y. Jing, J. Lin, J. Alloys Compd. 490 (2010) 684.
[20] A. Santana-Alonso, J. Mendez-Ramos, A.C. Yanes, J. del-Castillo, V.D. Rodriguez, Opt. Mater. 32 (2010) 903.
[21] C.X. Li, Z.W. Quan, J. Yang, P.P. Yang, J. Lin, Inorg. Chem. 46 (2007) 6329.
[22] C.Y. Cao, X.M. Zhang, M.L. Chen, W.P. Qin, J.S. Zhang, J. Alloys Compd. 505 (2010) 6.
[23] X. Wang, J. Zhuang, Q. Peng, Y.D. Li, Nature 437 (2005) 121.
[24] S.J. Zeng, G.Z. Ren, Q.B. Yang, J. Alloys Compd. 493 (2010) 476.
[25] S.J. Zeng, G.Z. Ren, Q.B. Yang, J. Mater. Chem. 20 (2010) 2152.
[26] S.J. Zeng, G.Z. Ren, W. Li, C.F. Xu, Q.B. Yang, J. Phys. Chem. C 114 (2010) 10750.
[27] A. Patra, Chem. Phys. Lett. 387 (2004) 35.
[28] F. Auzel, C. R. Acad. Sci. Paris 262 (1966) 1016.
[29] G. Qin, W. Qin, C. Wu, S. Huang, D. Zhao, J. Zhang, S. Lu, Opt. Commun. 242 (2004) 215.
[30] R.J. Thrash, L.F. Johnson, J. Opt. Soc. Am. B 11 (1994) 881.